AMERICAN SOCIETY FOR MICROBIOLOGY | Applied and Environmental Microbiology®

GEOMICROBIOLOGY

Uniform and Pitting Corrosion of Carbon Steel by *Shewanella oneidensis* MR-1 under Nitrate-Reducing Conditions

Robert B. Miller II,[a,b] Kenton Lawson,[c] Anwar Sadek,[c] Chelsea N. Monty,[c] John M. Senko[a,b,d]

[a]Department of Biology, The University of Akron, Akron, Ohio, USA
[b]Integrated Bioscience Program, The University of Akron, Akron, Ohio, USA
[c]Department of Chemical and Biomolecular Engineering, The University of Akron, Akron, Ohio, USA
[d]Department of Geosciences, The University of Akron, Akron, Ohio, USA

ABSTRACT Despite observations of steel corrosion in nitrate-reducing environments, processes of nitrate-dependent microbially influenced corrosion (MIC) remain poorly understood and difficult to identify. We evaluated carbon steel corrosion by *Shewanella oneidensis* MR-1 under nitrate-reducing conditions using a split-chamber/zero-resistance ammetry (ZRA) technique. This approach entails the deployment of two metal (carbon steel 1018 in this case) electrodes into separate chambers of an electrochemical split-chamber unit, where the microbiology or chemistry of the chambers can be manipulated. This approach mimics the conditions of heterogeneous metal coverage that can lead to uniform and pitting corrosion. The current between working electrode 1 (WE1) and WE2 can be used to determine rates, mechanisms, and, we now show, extents of corrosion. When *S. oneidensis* was incubated in the WE1 chamber with lactate under nitrate-reducing conditions, nitrite transiently accumulated, and electron transfer from WE2 to WE1 occurred as long as nitrite was present. Nitrite in the WE1 chamber (without *S. oneidensis*) induced electron transfer in the same direction, indicating that nitrite cathodically protected WE1 and accelerated the corrosion of WE2. When *S. oneidensis* was incubated in the WE1 chamber without an electron donor, nitrate reduction proceeded, and electron transfer from WE2 to WE1 also occurred, indicating that the microorganism could use the carbon steel electrode as an electron donor for nitrate reduction. Our results indicate that under nitrate-reducing conditions, uniform and pitting carbon steel corrosion can occur due to nitrite accumulation and the use of steel-Fe(0) as an electron donor, but conditions of sustained nitrite accumulation can lead to more-aggressive corrosive conditions.

IMPORTANCE Microbially influenced corrosion (MIC) causes damage to metals and metal alloys that is estimated to cost over $100 million/year in the United States for prevention, mitigation, and repair. While MIC occurs in a variety of settings and by a variety of organisms, the mechanisms by which microorganisms cause this damage remain unclear. Steel pipe and equipment may be exposed to nitrate, especially in oil and gas production, where this compound is used for corrosion and "souring" control. In this paper, we show uniform and pitting MIC under nitrate-reducing conditions and that a major mechanism by which it occurs is via the heterogeneous cathodic protection of metal surfaces by nitrite as well as by the microbial oxidation of steel-Fe(0).

KEYWORDS corrosion, nitrate reduction, nitrite, MIC, iron oxidation, biocorrosion

Microbially influenced corrosion (MIC) is the degradation of a material due to activities of microorganisms and has been estimated to cost a variety of industries in the United States up to $140 million annually in maintenance, prevention, and repairs (1, 2). MIC may occur by a variety of mechanisms, ranging from the direct

Received 4 April 2018 **Accepted** 6 April 2018
Accepted manuscript posted online 13 April 2018
Citation Miller RB, II, Lawson K, Sadek A, Monty CN, Senko JM. 2018. Uniform and pitting corrosion of carbon steel by *Shewanella oneidensis* MR-1 under nitrate-reducing conditions. Appl Environ Microbiol 84:e00790-18. https://doi.org/10.1128/AEM.00790-18.
Editor Frank E. Löffler, University of Tennessee and Oak Ridge National Laboratory

Address correspondence to John M. Senko, senko@uakron.edu.

microbial metabolism of metal to enhanced metal deterioration due to microbiologically induced changes in fluid chemistry (1, 3–5). While metal corrosion may occur in a variety of patterns, MIC most often results in a combination of uniform and pitting corrosion (3–13). Uniform corrosion involves the oxidation of the metal across its surface by a dissolved oxidant and results in mass loss from the metal (14, 15). Pitting corrosion is localized, and while it may result in relatively minor mass loss, it can result in a severe compromise of metal strength (14–16). Additionally, MIC can occur under a variety of terminal electron-accepting conditions. Waters containing high nitrate concentrations derived from agricultural sources, industrial wastewaters, wastewater treatment systems, and oil and gas production, containing nitrate at concentrations of 1 to 10 mM, may interact with a variety of steel structures (17–23). Notably, nitrate and nitrite are widely used in the oil and gas sectors to limit sulfate-reducing bacterial activities, which result in the corrosion of steel pipes and equipment and "souring" of petroleum (21–23). However, nitrate addition has also been suggested to enhance corrosion in such systems (e.g., see references 6 and 7).

MIC may occur via several mechanisms under nitrate-reducing conditions. First, nitrate may support thickened biofilms, thus inducing localized cathodic and anodic regions on the steel, with resultant pitting corrosion (3–5). Second, nitrite, an intermediate in dissimilatory nitrate reduction, may accumulate in fluids and oxidize Fe(0) in a uniform corrosion process, but localized nitrite accumulation can result in pitting (6). That said, nitrite is also frequently deployed as a corrosion inhibitor (21–23). Finally, nitrate may support the direct microbial metabolism of Fe(0) in steel or the consumption of cathodic H_2, both of which result in the oxidation of carbon steel-Fe(0) and often result in pitting (7–13). In light of the various potential mechanisms of MIC under nitrate-reducing conditions, we evaluated corrosion during nitrate reduction using *Shewanella oneidensis* MR-1 as a model nitrate-reducing bacterium in batch incubations and in a split-chamber/zero-resistance ammetry (ZRA) format (24, 25). *S. oneidensis* MR-1 reduces nitrate to ammonium, with a transient accumulation of nitrite (26). The split-chamber/ZRA approach entails the deployment of two metal working electrodes (referred to as WE1 and WE2) in the two chambers of an electrochemical split cell (here, we refer to "cells" as "chambers" to avoid confusion with bacterial cells). The working electrodes are connected by a short circuit, through a ZRA, and measurements can be collected in real time throughout the experiments. In these types of experiments, the magnitude and direction of electric current can be used to determine rates, mechanisms, and, we now show, extents of corrosion. We use this setup to mimic the heterogeneous biological and chemical conditions to which a metal might be exposed and that are responsible for corrosion, including pitting corrosion (3). We hypothesized two mechanisms of microbially mediated corrosion of carbon steel under nitrate-reducing conditions. The first mechanism for corrosion is due to nitrite accumulation during nitrate reduction, whereby nitrite oxidizes Fe(0). In the second mechanism, *S. oneidensis* oxidizes Fe(0) in steel to support nitrate and nitrite reduction.

RESULTS AND DISCUSSION

Overview of ZRA incubations. To evaluate the influence of nitrate-reducing bacterial activities on the corrosion of carbon steel, a series of ZRA incubations was conducted, in which carbon steel 1018 working electrodes were deployed in both of the split chambers. The conditions during the ZRA incubations are shown in Table 1, and results of this series of incubation experiments are shown in Fig. 1. Figure 1 (top) shows a timeline to indicate processes that we hypothesize to be occurring based on data obtained during the ZRA incubations, and these processes are depicted as P1 to P7 in Fig. 2. Before the initiation of experiments, WE1 and WE2 were immersed in identical solutions and with no inoculation or other experimental manipulation. During this period, minimal current was observed, indicating that the two chambers were in electrochemical equilibrium (Fig. 1). During this period, minor amounts of H^+ reduction (8, 27) were likely occurring to equal extents on both electrodes (Fig. 1 and 2, P1). Subsequently, amendments were made to either chamber of the split-chamber assem-

TABLE 1 Incubation conditions and weight loss of working electrodes in ZRA experiments

ZRA run	Chamber or electrode	Chamber components	Corrosion rate (mils/yr)
ZRA1 (blue)	WE1	15 mM lactate, 20 mM nitrate, inoculated	16
	WE2	15 mM lactate, 20 mM nitrate, no inoculation	65
ZRA2 (black)	WE1	15 mM nitrite, uninoculated	55
	WE2	15 mM nitrate, uninoculated	80
ZRA3 (pink)	WE1	15 mM lactate, inoculation and addition of 3 mM nitrite	16.1
	WE2	15 mM lactate, addition of 3 mM nitrite	39
ZRA4 (red)	WE1	20 mM nitrate, inoculated	79
	WE2	20 mM nitrate, no inoculation	102

blies to initiate the experiments, including inoculation with *S. oneidensis* or the addition of substrates. Control experiments were conducted, in which medium was contained in both chambers of a split-chamber assembly, and after 2 days of equilibration, lactate was added to the WE1 chamber. This resulted in minimal change in the current or potential in the WE1 chamber (see Fig. S1 in the supplemental material), indicating that electrochemical responses in ZRA incubations were not simply due to the addition of reagents.

Abiotic oxidation of carbon steel-Fe(0) by biogenic nitrite. For ZRA1, upon the addition of nitrate to WE1 and WE2 and *S. oneidensis* to WE1, a negative current developed, indicating electron transfer from WE2 to WE1 (Fig. 1 and 2, P3). The development of this negative current occurred concomitantly with an increase in the potential in the WE1 chamber, nitrate and lactate depletion, and nitrite accumulation (Fig. 1). Upon the complete depletion of nitrate, nitrite remained in WE1, and the magnitude of the current diminished but remained negative, suggesting that the remnant nitrite could be maintaining the current from WE2 to WE1 (Fig. 1 and 2, P6). With continued incubation, nitrite was depleted, and the negative current was diminished further (Fig. 1). Additionally, while both WE1 and WE2 experienced corrosion, the corrosion rate of WE2 was higher than that of WE1, with a corrosion rate ratio (WE1 to WE2) of 1:4 (Table 1). No current was observed in uninoculated and nitrite-free incubation mixtures, and the mass loss from coupons was $<$5 mg. To confirm the observations of corrosion under nitrate-reducing conditions, we conducted batch incubations that included carbon steel coupons in the same medium used for ZRA incubations. In incubation mixtures containing *S. oneidensis* and lactate, mass loss from coupons (indicative of uniform corrosion) occurred concurrently with nitrate depletion and nitrite accumulation but did not occur in uninoculated incubation mixtures (Fig. 3). Mass loss and accumulation of corrosion products in these experiments indicated that uniform corrosion was occurring, but surface topographic analysis of coupons from batch incubations also revealed the development of pits over the course of the incubations that were not observed after incubation in uninoculated medium (Fig. 4). As such, both uniform (as indicated by mass loss) and pitting corrosion occurred under nitrate-reducing conditions. Indeed, the dynamics of electron transfer and mass loss in ZRA incubations was consistent with the development of anodic and cathodic regions of metal surfaces (Fig. 2, P3, P5, and P6) that may lead to pitting corrosion.

The ZRA current patterns and the higher corrosion rate of WE2 than of WE1 in ZRA1 indicates that cathodic protection was occurring on WE1, with WE2 serving as the anode in a manner consistent with the mechanism of pitting corrosion (16). Based on these observations, we propose that during the period of lactate-dependent nitrate reduction, the accumulated nitrite served as an oxidant at WE1 (Fig. 1 and 2, P3), with WE2 serving as the "sacrificial" electrode. Subsequently, remnant nitrite continued to cathodically protect WE1, and the current remained negative (Fig. 1 and 2, P6). However, it is not clear if nitrite interacted directly with Fe(0) in the steel (reaction 1 [R1]) or if nitrite reacted with Fe(II) from cathodic H^+ reduction (R2 and R3), thus facilitating further Fe(0) oxidation: $3\ Fe^0 + 2\ NO_2^- + 8\ H^+ \rightarrow 3\ Fe^{2+} + N_2 + 4\ H_2O$

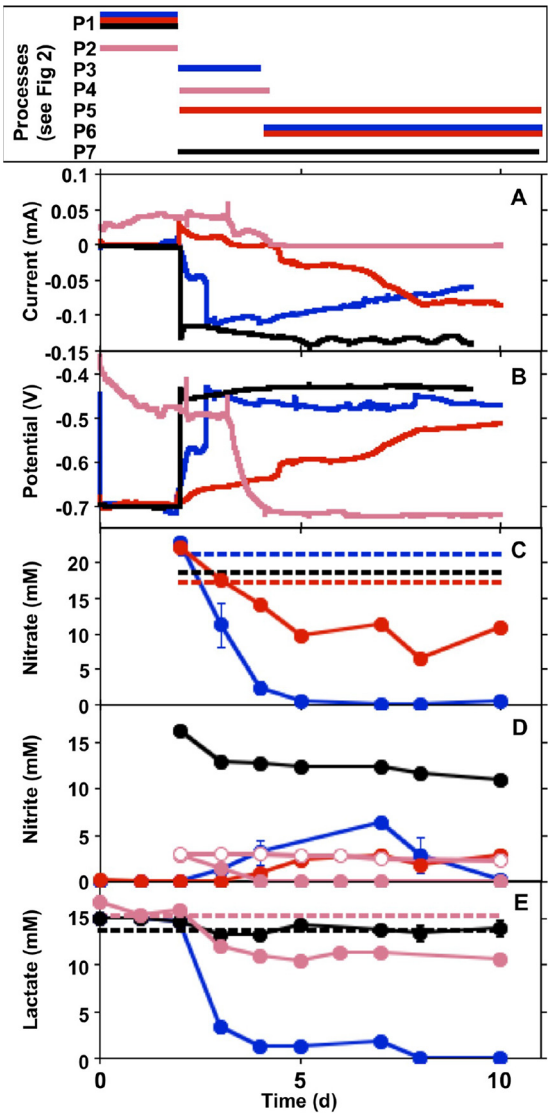

FIG 1 Current (A), potential (in the WE1 chamber versus a standard calomel electrode) (B), nitrate concentrations (C), nitrite concentrations (D), and lactate concentrations (E) in incubation mixtures with *S. oneidensis* and carbon steel coupons deployed in the WE1 and WE2 chambers of split chambers connected by ZRA. Data for incubations designated ZRA1, ZRA2, ZRA3, and ZRA4 (shown in Table 1) are depicted by blue, black, pink, and red lines or shapes, respectively. All data depicted with closed shapes indicate nitrate, nitrite, or lactate concentrations in WE1. Open circles in panel D represent nitrite concentrations in WE2. Dashed lines represent mean concentrations of nitrate or lactate measured in WE2. Error bars represent one standard deviation of data from triplicate incubations. The box at the top indicates the time periods of processes (shown in Fig. 2) associated with each type of incubation.

(0.33 V) (R1), $Fe^0 + 2\ H^+ \rightarrow Fe^{2+} + H_2$ (0.22 V) (R2), and $6\ Fe^{2+} + 2\ NO_2^- + 14\ H_2O \rightarrow 6\ Fe(OH)_3 + N_2\ 10\ H^+$ (0.08 V) (R3).

While there are instances of direct attack of Fe(0) by nitrite (28–30), Fe(II) oxidation by nitrite is well established and is enhanced in the presence of solid phases (31–35). We also point out that the choice of N_2 as the product of nitrite reduction in R1 and R3 was arbitrary, since these products are not well known (34, 35). N_2O may be the product of nitrite reduction by Fe(II) (35), and ammonium may be a product of nitrite reduction by Fe(0) (7). Ultimately, Fe(0) oxidation by nitrite may be due to a combination of R1 and R3 (Fig. 2, P3).

To test the hypothesis that nitrite serves to oxidize Fe(0) in carbon steel, we conducted ZRA incubations (ZRA2), during which nitrite was added to the WE1 chamber, without any inoculum. Upon the addition of nitrite, we observed the development

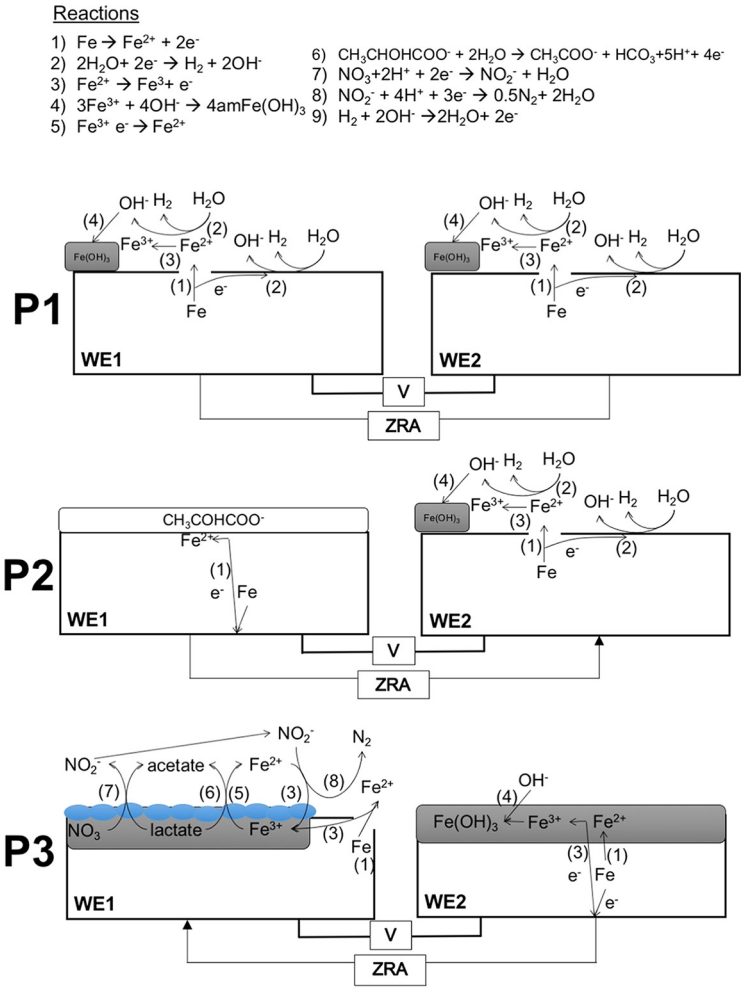

FIG 2 Schematic representations of reactions proposed to be occurring during ZRA experiments shown in Fig. 1. Numbers shown in parentheses next to arrows indicate the proposed reactions shown at the top. Blue ovals represent *S. oneidensis* cells. Arrows on ZRA lines indicate the direction of electron transfer, as indicated by current in Fig. 1. Amorphous Fe(III) (hydr)oxide is depicted as $amFe(OH)_3$.

of a negative current and an increase in the potential in the WE1 chamber that were similar to what was observed for the ZRA1 incubations (Fig. 1). This indicates that nitrite served as an oxidant at the WE1 cathode, with WE2 serving as the anode (Fig. 1 and 2, P7). It is also notable that the current remained constant throughout the ZRA2 incubations, since the nitrite concentration remained high throughout the incubations. This is in contrast to the ZRA1 incubations, in which nitrite transiently accumulated and was ultimately depleted by *S. oneidensis* (Fig. 1D). We also observed a higher corrosion rate for WE2 than for WE1, with a corrosion rate ratio of 1:1.5 (Table 1). These results are again consistent with a mechanism for pitting corrosion, whereby localized anodes and cathodes develop on metal surfaces as a result of microbiological activities.

Influence of nitrite concentration on carbon steel corrosion. While nitrite is frequently used as a corrosion inhibitor (36–38), it is also a strong oxidant, and the inhibition or enhancement of carbon steel corrosion by nitrite appears to be concentration dependent (7). To confirm that nitrite induced carbon steel corrosion and evaluate the influence of the nitrite concentration on the abiotic oxidation of Fe(0), we determined the mass loss of coupons included in nitrite-amended growth medium. We observed mass loss from coupons in uninoculated medium with 6 mM and 3 mM nitrite, but the mass loss in 1 mM nitrite-containing incubation mixtures was indistinguishable from that of nitrite-free controls (Fig. 5A to C). Mass loss was most extensive

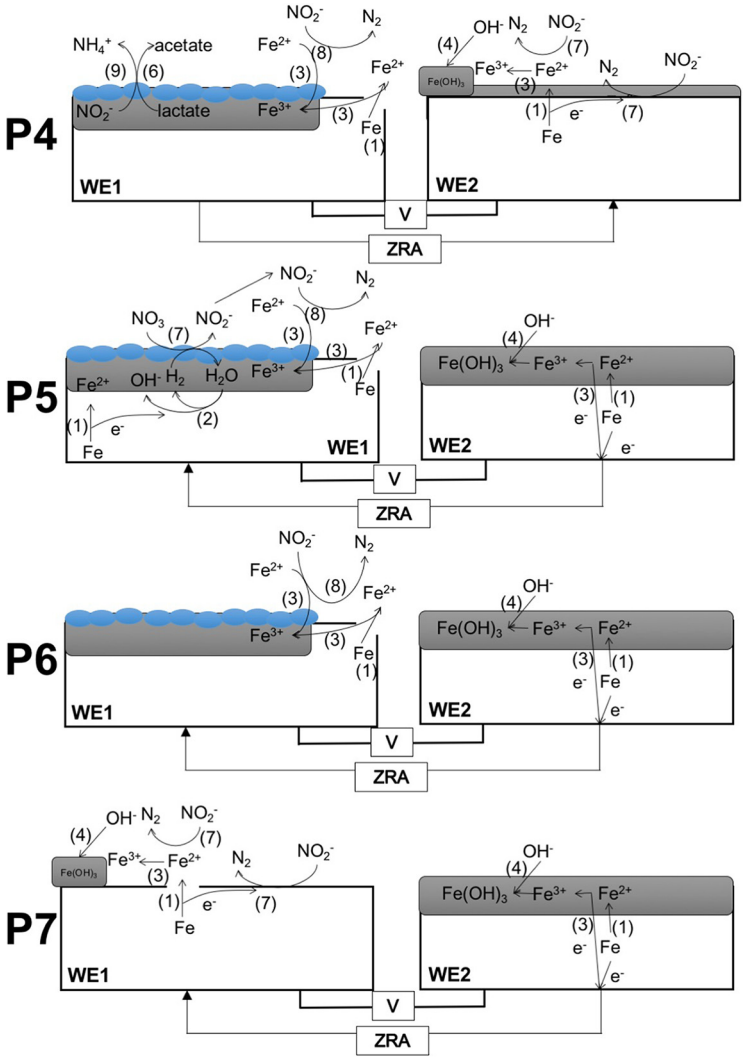

FIG 2 (Continued)

in incubations with 6 mM nitrite (Fig. 5A to C). Additionally, we observed nitrite depletion concurrent with mass loss (Fig. 5D to F), indicating that the Fe(0) oxidation and mass loss were due to nitrite. When *S. oneidensis* was included in medium with 6 mM nitrite, the mass loss was the same as that observed in uninoculated incubation mixtures (Fig. 5A), since nitrite remained in the incubation mixtures, and the most extensive mass loss in incubations with *S. oneidensis* and 6 mM nitrite appeared to occur when the nitrite concentration was >1 mM (Fig. 5A and D). A similar 1 mM "threshold" nitrite concentration was observed in incubation mixtures that included *S. oneidensis* and 3 mM nitrite (Fig. 5B and E), and carbon steel corrosion in the presence of *S. oneidensis* and 1 mM nitrite was not distinguishable from that in nitrite-free control incubation mixtures (Fig. 5F). These observations indicate that the abiotic oxidation of carbon steel-Fe(0) by nitrite is concentration dependent, and in batch incubations, biological and abiotic corrosion in the presence of nitrite proceeded to similar extents.

We also conducted ZRA incubations in which 3 mM nitrite was included in lactate-amended medium (ZRA3) (Table 1). Under these conditions, a slightly positive current occurred before the addition of nitrite and *S. oneidensis* (Fig. 1A). This was likely due to slight differences in the coupon surface roughness, lactate concentration, or pH in the WE1 and WE2 chambers (39). Upon the addition of nitrite and *S. oneidensis* to the WE1 chamber, the current diminished concurrently with nitrite consumption (Fig. 2, P4) until

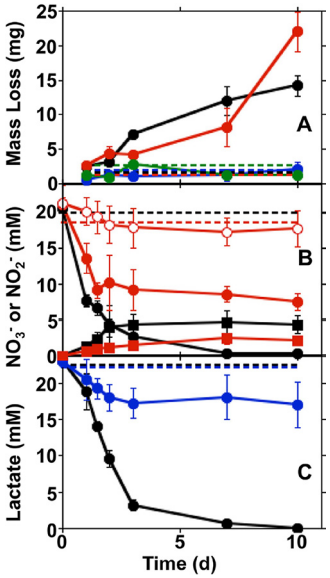

FIG 3 Steel coupon mass loss (A), nitrate and nitrite concentrations (B), and lactate concentrations (C) in incubations of *S. oneidensis* and carbon steel coupons in minimal medium containing nitrate and lactate (black), nitrate (red), lactate (blue), or no nitrate or lactate (green). Dashed lines represent mean mass losses and concentrations of nitrate or lactate in uninoculated medium. Closed circles and squares in panel B represent nitrate and nitrite concentrations, respectively. Open circles in panel B represent nitrate concentrations in incubations of *S. oneidensis* in medium containing nitrate but no steel coupon or lactate. Error bars represent one standard deviation of data from triplicate incubations.

no current was observed (Fig. 1A), indicating that the electrodes were in equilibrium. These observations indicated that if nitrite was consumed, its corrosive effect would be limited. Additionally, in ZRA incubations, we found that there was a strong correlation between the difference in mass losses between WE1 and WE2 and the difference in maximal nitrite concentrations between WE1 and WE2 chambers (Fig. 6). In other words, the greater the nitrite accumulation in the WE1 chamber, the more mass was lost from WE2. These mass loss values were consistent with theoretical mass losses predicted from Faraday's law (Fig. 6). The inability of the split-chamber/ZRA approach to quantify mass loss has been noted (40), but these new observations indicate that the approach may be exploited to quantify extents of corrosion. In this case, the total charge passed during the experiment was calculated by using the trapezoid rule to integrate the area under the current-versus-time plots from ZRA incubations (Fig. 1). Taken together, these results indicate that the extent of corrosion is directly dependent on the concentration of nitrite.

Nitrate-dependent oxidation of carbon steel-Fe(0) by *S. oneidensis*. While nitrite clearly induced the oxidation of Fe(0) and the resultant carbon steel corrosion, this reaction could also be attributable to metabolic oxidative processes by *S. oneidensis* and coupled to nitrate reduction. For instance, under sulfate-reducing conditions, Fe(0) may be oxidized when cathodic H_2 (R2) is consumed by hydrogenotrophic sulfate-reducing bacteria (41), and H_2 could be similarly consumed under nitrate-reducing conditions (7, 9, 12, 42, 43): $4\ H_2 + NO_3^- + 2\ H^+ \rightarrow NH_4^+ + 3\ H_2O$ (biological) (R4).

Similarly, Fe(0) in steel may be directly (i.e., "enzymatically") oxidized under anoxic conditions (10, 13, 43–45) (depicted using nitrate reduction in R5): $4\ Fe^0 + NO_3^- + 10\ H^+ \rightarrow 4\ Fe^{2+} + NH_4^+ + 3\ H_2O$ (biological) (R5).

The latter mechanism of Fe(0) oxidation poses a challenge to microorganisms, in that they must use a solid phase as an electron donor (13). However, *Shewanella* spp. can use poised graphite cathodes as electron donors, so they are a group of organisms capable of using insoluble electron donors as well as acceptors (33, 46–48). While it is not known if *S. oneidensis* can oxidize Fe(II) under nitrate-reducing conditions, *Shewanella* spp. may oxidize Mn(II) under aerobic conditions (49). As such, R2 might be

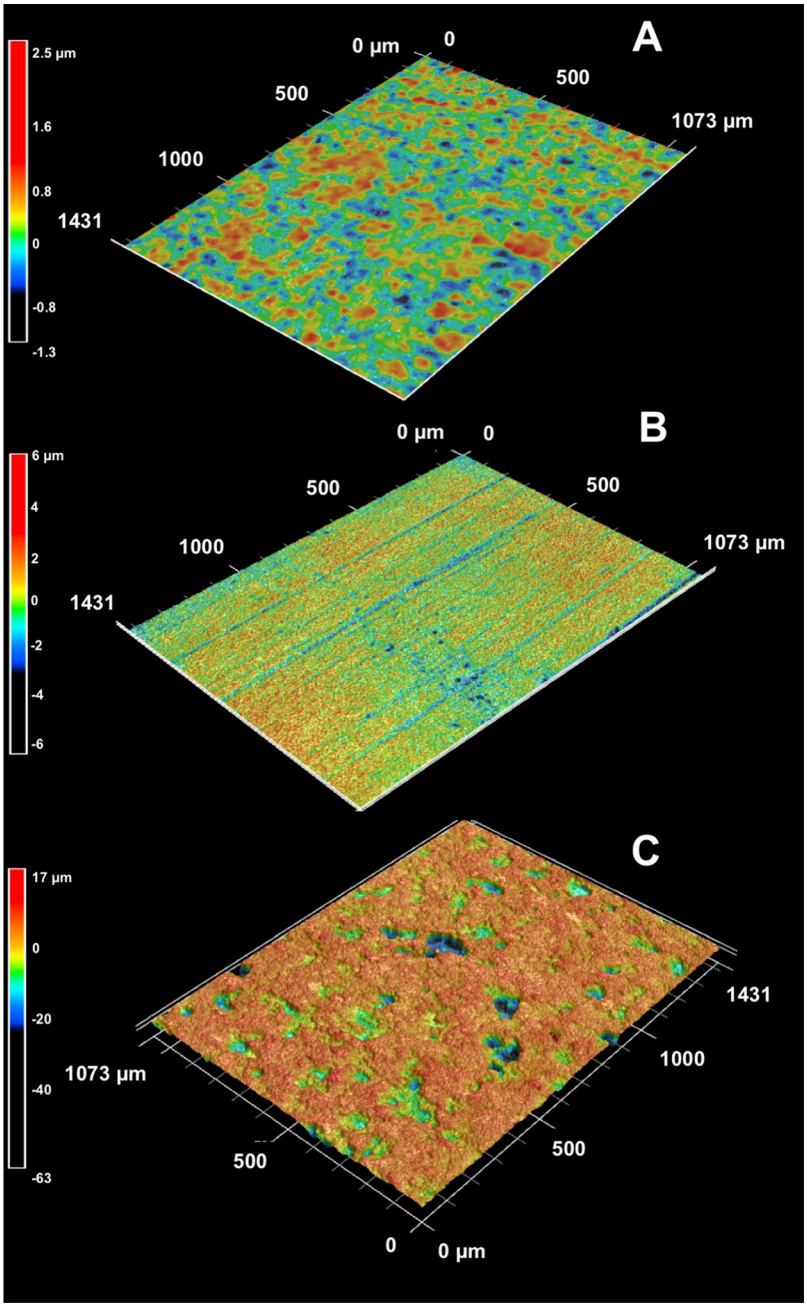

FIG 4 Surface topographic characteristics of carbon steel coupons incubated in uninoculated medium for 10 days (A) and with *S. oneidensis* under lactate-oxidizing, nitrate-reducing conditions for 5 days (B) and 60 days (C). Heat map scales are shown next to their corresponding topographic maps.

facilitated by nitrate-dependent Fe(II) oxidation by *S. oneidensis*. Regardless of the specific mechanism of carbon steel-Fe(0) oxidation, the above-described scenarios describe the use of Fe(0)-derived electrons to support nitrate reduction.

To test the hypothesis that Fe(0) oxidation (whether via R4 or R5) could be coupled to nitrate reduction by *S. oneidensis*, we conducted ZRA4, in which no lactate was included in the growth medium, and the WE1 chamber was inoculated with *S. oneidensis* (Table 1). Under these conditions, the only potential electron donor available to the cells is the Fe(0) in the carbon steel coupon. Upon inoculation of the WE1 chamber, a negative current gradually developed, with a concurrent increase in the potential in the WE1 chamber (Fig. 1A and B). The negative current indicated that WE1 was serving

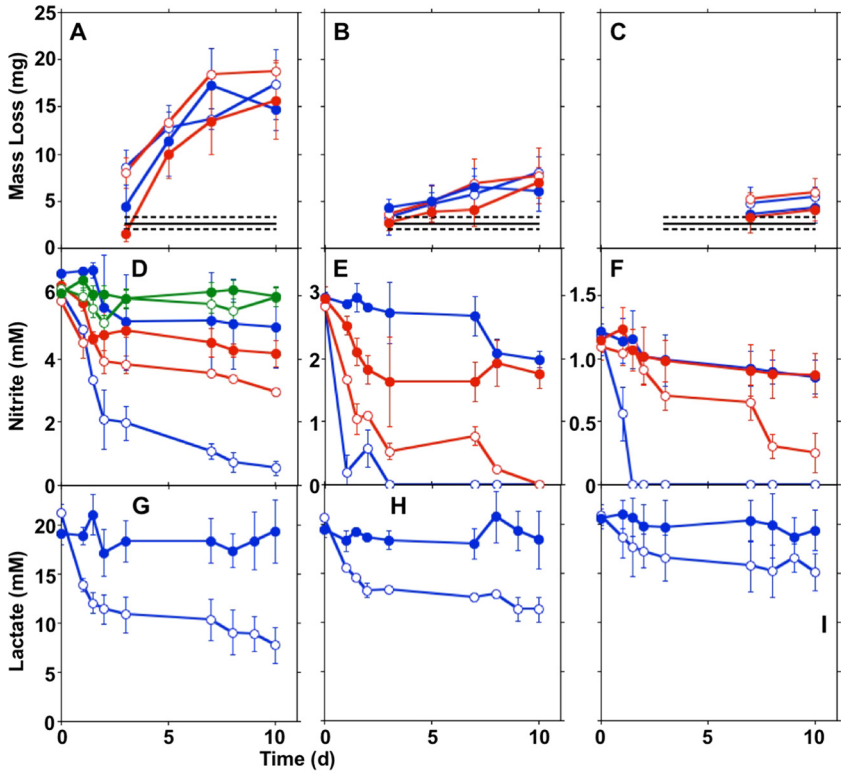

FIG 5 Steel coupon mass loss (A to C), nitrite concentrations (D to F), and lactate concentrations (G to I) in incubations of carbon steel coupons in minimal medium with 6 mM (A, D, and G), 3 mM (B, E, and H), or 1 mM (C, F, and I) nitrite with (blue) or without (red) lactate amendment. Green shapes in panel C show nitrite concentrations in incubation mixtures that did not contain steel coupons. Open shapes indicate incubation mixtures that included *S. oneidensis*, and closed shapes indicate uninoculated incubation mixtures. Error bars represent one standard deviation of data from triplicate incubations.

as the cathode in the split chamber, while WE2 was serving as the anode (Fig. 1 and 2, P5). This redox disequilibrium between electrodes was due to the activities of *S. oneidensis*. This conclusion is supported by the greater mass loss of WE2 than of WE1 at the conclusion of ZRA4 (Table 1). Additionally, nitrate consumption was observed, which indicated that Fe(0) was serving as an electron donor to support nitrate reduction by *S. oneidensis* (Fig. 1C). However, nitrite also accumulated in the incubation mixtures (Fig. 1D), which may have also oxidized Fe(0) (R1 and R3) (Fig. 2).

Similar to the ZRA4 incubations, in batch incubations, carbon steel supported nitrate reduction by *S. oneidensis* in lactate-free medium that was not observed the absence of the coupon (Fig. 3B), indicating that remnant reducing equivalents from cell cultivation before the incubations were not sustaining nitrate reduction (Fig. 3B). Rather, nitrate reduction was supported by Fe(0) oxidation, as we also observed mass loss from the steel coupons with these incubations (Fig. 3A). We point out that nitrite accumulated in these incubation mixtures (Fig. 3B), so it is difficult to determine if the observed Fe(0) oxidation is attributable exclusively to the biological oxidation of the metal. That said, Fe(0) must have served as an electron donor to support nitrate reduction and nitrite accumulation, so the corrosion that we observed was at least partially attributable to Fe(0) oxidation by *S. oneidensis* and not nitrite. Steel coupons also supported nitrite reduction in lactate-free batch incubations where nitrite was provided as the electron acceptor (Fig. 5A and B), and mass loss from these coupons was also observed (Fig. 5D and E). Similar to incubation mixtures that included nitrate, nitrite reduction was more extensive in lactate-free incubation mixtures that included coupons than in those that did not include coupons (Fig. 5D), indicating that the nitrate reduction was not attributable to excess reducing equivalents carried over with tryptic soy broth (TSB)-grown *S. oneidensis*.

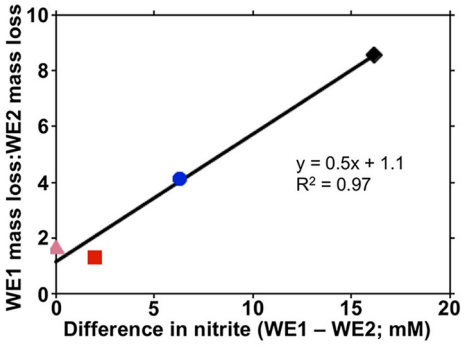

ZRA run	Symbol	Difference in Mass loss (WE1-WE2)	Predicted difference in mass loss	Efficiency (%)
ZRA1	●	-49 mg	-41 mg	82%
ZRA2	◆	-23 mg	-20 mg	88%
ZRA3	▲	-11 mg	-9.5 mg	90%
ZRA4	■	-23 mg	-20 mg	88%

FIG 6 Relationship between differences in maximal nitrite concentrations in WE1 and WE1 chamber fluid and ratios of mass loss from these electrodes. The table provides the key for the figure and comparison of measured and predicted mass loss differences between WE1 and WE2. Predicted mass losses were calculated based on the total measured current over the course of the experiments and Faraday's law. See the text for details on calculations.

Implications for corrosion prevention and mitigation. Nitrate is frequently used to control MIC (mostly MIC attributable to sulfate-reducing bacterial activities) and souring of crude oil (21, 22, 50). The work presented here as well as elsewhere illustrates the potential for both uniform and pitting corrosion of carbon steel under nitrate-reducing conditions. For instance, Li et al. (51) suggested that nitrate-dependent Fe(II)-oxidizing bacteria may induce the corrosion of carbon steel. More specifically, *Bacillus licheniformis* has been shown to induce pitting under nitrate-reducing conditions (11), but uniform corrosion was not evaluated. Additionally, an organic carbon source was provided in the incubation mixtures (11), so it is difficult to determine the relative contributions of biogenic nitrite and nitrate-dependent Fe(0) oxidation to the overall process of corrosion. Similarly, the nitrate-dependent, Fe(II)-oxidizing organism *Dechloromonas hortensis* enhanced the corrosion of cast iron, but it is not clear if this organism could directly oxidize Fe(0) (52). A non-hydrogen-consuming *Prolixibacter* sp. was shown to induce Fe(0) oxidation and corrosion under nitrate-reducing conditions, indicating that Fe(0) may be directly metabolized [i.e., without an H_2 or Fe(II) intermediate], coupled to nitrate reduction (12, 43). However, those studies did not specifically evaluate pitting or uniform corrosion (12, 43). Finally, nitrite may abiotically oxidize Fe(0) (30).

Taken together, these observations illustrate the diversity of mechanisms by which microorganisms can induce the corrosion of carbon steel. Indeed, our work indicates that microorganisms induce corrosion by using Fe(0) as an electron donor to support nitrate and nitrite reduction. The mechanism by which *S. oneidensis* oxidizes Fe(0) remains unclear. Work by De Windt et al. (8) indicated that *S. oneidensis* used cathodic H_2 to oxidize Fe(0) coupled with nitrate reduction. Those authors used N_2O production as an indicator of nitrate reduction, but ammonium is the terminal product of nitrate reduction by *S. oneidensis* MR-1 (without N_2O as an intermediate) (26, 53), and biogenic nitrite may have been reduced to N_2O by Fe(0) in those experiments. As such, the extent to which nitrite induced Fe(0) oxidation in those experiments is unclear. Additionally, the relevance Fe(0) oxidation driven by cathodic H_2 oxidation as a mechanism of MIC has been questioned due to kinetic considerations, and mounting evidence indicates that direct oxidation of the metal is the principal means by which microorganisms use Fe(0) as an electron donor (e.g., see references 10, 13, and 54).

Besides using Fe(0) in carbon steel as an electron donor to support nitrate and nitrite reduction, when organic carbon is present to support nitrate reduction, nitrite that accumulates abiotically reacts with Fe(0) to induce corrosion. In our experiments, MIC during lactate-supported nitrate reduction occurred more rapidly and to a greater extent than in the absence of lactate (Fig. 1 and Table 1). Additionally, denitrification and dissimilatory nitrate reduction to ammonium are nearly ubiquitous processes (and potential processes) in near-surface soils and sediments (55–57). As such, corrosion by nitrite attack might be a more widespread form of MIC under nitrate-reducing conditions. That said, the prevalence of Fe(0)-oxidizing, nitrate-reducing microorganisms remains unclear. The finding of carbon steel corrosion by nitrite is somewhat surprising, as nitrite has been used as a corrosion inhibitor, because it induces the development of a passive Fe(III) film on steel (36–38, 58). For instance, Kielemoes et al. (7) presented evidence that relatively high concentrations (≥2 mM) of nitrite inhibited corrosion, while nitrate concentrations below this threshold enhanced corrosion. However, nitrite has been shown to either enhance or inhibit corrosion, depending on nitrite and chloride ratios (7, 36, 37). The observation of corrosion inhibition by nitrite may be an artifact of conducting experiments with homogenous solutions, whereby uniform "coverage" of metal surfaces by nitrite cathodically protects the metal from further corrosion. If this same protection is heterogeneous, as is the case in ZRA incubations, the redox imbalance between regions of the metal surface may induce more-aggressive corrosion (e.g., WE1 was protected by nitrite, while WE2 was oxidized) (Fig. 2, P7).

Our results indicate two processes under nitrate-reducing conditions that lead to pitting and uniform corrosion. In batch incubations, the mass loss from coupons indicated uniform corrosion under nitrate-reducing conditions. Pitting corrosion also occurred in the incubation mixtures, as evidenced by surface profiling of coupons. The ZRA incubations presented here mimic the conditions that would lead to pitting corrosion: different redox conditions on the metal surface. Under these conditions, heterogeneous biofilm coverage of metal surfaces by nitrate-reducing microorganisms could lead to localized electron biological "extraction" of electrons under conditions of low organic carbon concentrations or localized accumulations of nitrite under conditions where an organic electron donor is available to support nitrite reduction. In both cases, a localized cathode develops in proximity to, and as a result of, nitrate-reducing activities, with an anode at the adjacent uncovered surface. Additionally, in this work, we were able to compare the relative contributions of carbon steel-Fe(0) oxidation by nitrite and nitrate-dependent oxidation of carbon steel-Fe(0). Results from our ZRA experiments indicate that corrosion and current were more extensive during lactate-dependent nitrate reduction with nitrite accumulation than under lactate-free conditions. Given this observation and the widespread occurrence of organotrophic nitrate-reducing bacteria, nitrite-induced corrosion may be the predominant mechanism of MIC under nitrate-reducing conditions.

MATERIALS AND METHODS

Bacterial cultivation. *Shewanella oneidensis* MR-1 was routinely grown on a solid or liquid tryptic soy medium (TSB or tryptic soy agar [TSA]) consisting of tryptic soy powder (20 g/liter) and Bacto agar (15 g/liter for solid medium). Experiments were conducted in an anoxic minimal medium used previously by Myers and Nealson (59), which includes 9.0 mM $(NH_4)_2SO_4$, 5.7 mM K_2HPO_4, 3.3 mM KH_2PO_4, 2.0 mM $NaHCO_3$, 1.0 mM $MgSO_4$, 0.5 mM $CaCl_2$, 0.05 g/liter yeast extract, 0.1 g/liter Casamino Acids, 20 mg/liter L-arginine–HCl, 20 mg/liter L-glutamate, vitamins, and trace metals, as described previously by Tanner (60). The medium was buffered (pH 7.4) with HEPES, and sodium lactate (15 mM) was provided as an electron donor, where appropriate. To remove O_2 from the medium, the medium was brought to a boil and then cooled under a continuous stream of N_2. Sodium nitrate and sodium nitrite were provided to different media at various concentrations, depending on the type of experiment. In preparation for experimental incubations, *S. oneidensis* was grown on TSB to late log phase at room temperature and then harvested by centrifugation, washed with lactate-free minimal medium (see above), and resuspended in the same medium. *S. oneidensis* growth was determined by using optical density measurements at 600 nm in a Helios UV-visible (UV-Vis) spectrophotometer.

Corrosion incubations. Carbon steel (UNSG10180) samples were polished using progressively finer SiC papers, including 240, 320, 400, and 600 grit, as described in ASTM standard E1558 (61). Samples were weighed and then sterilized at 160°C for 4 h in a glass chamber filled with N_2 (62). This sterilization process minimizes the alteration of the metal surface that occurs during other standard sterilization

procedures (62). For batch experiments, flat steel coupons were aseptically placed in 160 ml in serum bottles with 50 ml of anoxic minimal medium and N_2 headspace. Serum bottles were sealed with thick butyl rubber stoppers with aluminum crimp seals. Where appropriate, sodium nitrate or sodium nitrite was added to media from sterile, anoxic stock solutions. TSB-grown *S. oneidensis* was added to minimal medium at an optical density at 600 nm of 0.8 and incubated at 22°C in darkness. Samples were periodically recovered to characterize fluid chemistry. Cells were removed from the suspension via centrifugation, and lactate, nitrate, and nitrite concentrations in the supernatant were measured (described below). Samples for lactate measurements were acidified with 0.008 N H_2SO_4.

To evaluate carbon steel corrosion in the split-chamber format with zero-resistance ammetry measurements (referred to as "ZRA incubations") (25), two glass chambers were assembled with polished, cylindrical working electrodes (referred to as WE1 and WE2; exposed area of 0.5 cm^2) inserted into each chamber of the split-chamber assembly. Assembled split chambers were sterilized as described above. A cation exchange membrane (catalog number CMI-7000S; Membranes International Inc., Ringwood, NJ) was primed in sterile 5% NaCl at 40°C for 24 h and then aseptically inserted between the two chambers. Both chambers were filled with 250 ml of sterile minimal medium, and a saturated calomel reference electrode (SCE) was inserted into the chamber containing WE1. Current and potential were measured by using a Gamry reference 600 potentiostat/galvanostat in ZRA mode. In this configuration, a positive current represents electron transfer from WE1 to WE2. To confirm the sign convention for the current, experiments were conducted with the galvanic couple of Al and Cu, where Al served as WE1 and Cu served as WE2. The resulting galvanic current from this experiment was positive, verifying our sign convention for current. Potential and current readings were collected at 5-min intervals during each ZRA incubation. For experiments that included bacterial cells, chamber WE1 received an inoculum of *S. oneidensis* at a cell density of 0.783. Samples were periodically removed from both chambers of the split-chamber apparatus to measure pH and lactate, nitrate, and nitrite concentrations (described below). At the conclusion of batch and ZRA incubations, the steel coupons were removed and subjected to weight loss analysis (WLA) (described below).

Analytical techniques. The lactate concentration was quantified by high-performance liquid chromatography (HPLC) using an Agilent 1200 series HPLC system (Agilent Technologies Inc., Santa Clara, CA) with an Aminex HPX-87H column (300 mm by 7.8 mm; Bio-Rad Laboratories Inc., Hercules, CA) with UV (230 nm) detection. A mobile phase of 0.008 N H_2SO_4 was used at a flow rate of 0.6 ml/min. Nitrate and nitrite concentrations were quantified by ion chromatography (DX 100; Dionex Corp., Sunnyvale, CA). Before topographic analysis of carbon steel coupons, the coupons were washed as described below, topographic features were visualized by using a Keyence VK-X250 three-dimensional (3D) laser microscope (Keyence Corp., Osaka, Japan), and data were analyzed by using the Keyence VK-X MultiFile analyzer.

Corrosion rates were determined by WLA according to ASTM method G01-03 (63). Steel coupons were rinsed with deionized water, brushed, and immersed in Clarke's reagent (1,000 ml 12.1 M HCl, 20 g antimony trioxide, and 50 g stannous chloride) at 30-s intervals to remove surface oxides. After the bath in Clarke's reagent, the coupons were rinsed with ultrapure water, dried, and weighed. This washing procedure was repeated until no further mass loss occurred between wash cycles, indicating the all oxides were removed. The corrosion rate was calculated by using the equation $CR = (W \times K)/(D \times A \times t)$, where CR represents corrosion rate in mils per year; K is a dimensionless constant, 3.45×10^6; W is the mass loss in grams; A is the exposed surface area in square centimeters; t is the exposure time in hours; and D is the density of carbon steel UNSG10180 in grams per cubic centimeter (63).

SUPPLEMENTAL MATERIAL

Supplemental material for this article may be found at https://doi.org/10.1128/AEM.00790-18.

SUPPLEMENTAL FILE 1, PDF file, 0.1 MB.

ACKNOWLEDGMENTS

This work was supported by the U.S. Department of Defense Office of Corrosion Policy and Oversight and the U.S. Air Force Academy (FY11-TCC9 and FY12-TCC4). The funders had no role in study design, data collection and analysis, decision to publish, or preparation of the manuscript.

We thank Wendy Goodson at the U.S. Air Force Research Laboratory for access to the 3D microscopy facility.

REFERENCES

1. Little BJ, Lee JS. 2007. Microbiologically influenced corrosion, 1st ed. Wiley, Hoboken, NJ.
2. Flemming H-C. 1996. Economical and technical overview, p 6–14. *In* Heitz E, Flemming H-C, Sands W (ed), Microbially influenced corrosion of materials. Springer-Verlag, New York, NY.
3. Beech IB. 2004. Corrosion of technical materials in the presence of biofilms—current understanding and state-of-the art methods of study. Int Biodeterior Biodegradation 53:177–183. https://doi.org/10.1016/S0964-8305(03)00092-1.
4. Beech IB, Sunner J. 2004. Biocorrosion: towards understanding interactions between biofilms and metals. Curr Opin Biotechnol 15:181–186. https://doi.org/10.1016/j.copbio.2004.05.001.

5. Videla HA, Herrera LK. 2005. Microbiologically influenced corrosion: looking to the future. Int Microbiol 8:169–180.
6. Lin K-S, Chang N-B, Chuang TD. 2008. Fine structure characterization of zero-valent iron nanoparticles for decontamination of nitrites and nitrates in wastewater and groundwater. Sci Technol Adv Mater 9:25015. https://doi.org/10.1088/1468-6996/9/2/025015.
7. Kielemoes I, De Boever P, Verstraete W. 2000. Influence of denitrification on the corrosion of iron and stainless steel powder. Environ Sci Technol 34:663–671. https://doi.org/10.1021/es9902930.
8. De Windt W, Boon N, Siciliano SD, Verstraete W. 2003. Cell density related H_2 consumption in relation to anoxic Fe(0) corrosion and precipitation of corrosion products by *Shewanella oneidensis* MR-1. Environ Microbiol 5:1192–1202. https://doi.org/10.1046/j.1462-2920.2003.00527.x.
9. Venzlaff H, Enning D, Srinivasan J, Mayrhofer KJJ, Hassel AW, Widdel F, Stratmann M. 2013. Accelerated cathodic reaction in microbial corrosion of iron due to direct electron uptake by sulfate-reducing bacteria. Corros Sci 66:88–96. https://doi.org/10.1016/j.corsci.2012.09.006.
10. Enning D, Garrelfs J. 2014. Corrosion of iron by sulfate-reducing bacteria: new views of an old problem. Appl Environ Microbiol 80:1226–1236. https://doi.org/10.1128/AEM.02848-13.
11. Xu D, Li Y, Song F, Gu T. 2013. Laboratory investigation of microbiologically influenced corrosion of C1018 carbon steel by nitrate reducing bacterium *Bacillus licheniformis*. Corros Sci 77:385–390. https://doi.org/10.1016/j.corsci.2013.07.044.
12. Iino T, Ito K, Wakai S, Tsurumaru H, Ohkuma M, Harayama S. 2015. Iron corrosion induced by nonhydrogenotrophic nitrate-reducing *Prolixibacter* sp. strain MIC1-1. Appl Environ Microbiol 81:1839–1846. https://doi.org/10.1128/AEM.03741-14.
13. Kato S. 2016. Microbial extracellular electron transfer and its relevance to iron corrosion. Microb Biotechnol 9:141–148. https://doi.org/10.1111/1751-7915.12340.
14. Gabrielli C, Keddam M. 1992. Review of applications of impedance and noise analysis to uniform and localized corrosion. Corrosion 48:794–811. https://doi.org/10.5006/1.3315878.
15. Melchers RE. 1999. Corrosion uncertainty modelling for steel structures. J Constr Steel Res 52:3–19. https://doi.org/10.1016/S0143-974X(99)00010-3.
16. Wang Y, Cheng G, Li Y. 2016. Observation of the pitting and uniform corrosion for X80 steel in 3.5 wt.% NaCl solutions using *in-situ* and 3-D measuring microscope. Corros Sci 111:508–517. https://doi.org/10.1016/j.corsci.2016.05.037.
17. Prakasa Rao EVS, Puttanna K. 2000. Nitrates, agriculture and environment. Curr Sci 79:1163–1168.
18. Ruiz G, Jeison D, Chamy R. 2003. Nitrification with high nitrite accumulation for the treatment of wastewater with high ammonia concentration. Water Res 37:1371–1377. https://doi.org/10.1016/S0043-1354(02)00475-X.
19. Tang C, Chen J, Shindo S, Sakura Y, Zhang W, Shen Y. 2004. Assessment of groundwater contamination by nitrates associated with wastewater irrigation: a case study in Shijiazhuang region, China. Hydrol Process 18:2303–2312. https://doi.org/10.1002/hyp.5531.
20. Korostynska O, Mason A, Al-Shamma'a A. 2012. Monitoring of nitrates and phosphates in wastewater: current technologies and further challenges. Int J Smart Sens Intell Syst 5:149–176. https://doi.org/10.21307/ijssis-2017-475.
21. Hubert C, Voordouw G. 2007. Oil field souring control by nitrate-reducing *Sulfurospirillum* spp. that outcompete sulfate-reducing bacteria for organic electron donors. Appl Environ Microbiol 73:2644–2653. https://doi.org/10.1128/AEM.02332-06.
22. Gieg LM, Jack TR, Foght JM. 2011. Biological souring and mitigation in oil reservoirs. Appl Microbiol Biotechnol 92:263–282. https://doi.org/10.1007/s00253-011-3542-6.
23. Dronen K, Roalkvam I, Beeder J, Torsvik T, Steen IH, Skauge A, Liengen T. 2014. Modeling of heavy nitrate corrosion in anaerobe aquifer injection water biofilm: a case study in a flow rig. Environ Sci Technol 48:8627–8635. https://doi.org/10.1021/es500839u.
24. Iannuzzi M, Kovac J, Frankel GS. 2007. A study of the mechanisms of corrosion inhibition of AA2024-T3 by vanadates using the split cell technique. Electrochim Acta 52:4032–4042. https://doi.org/10.1016/j.electacta.2006.11.019.
25. Miller RB, II, Sadek A, Rodriguez A, Iannuzzi M, Giai C, Senko JM, Monty CN. 2016. Use of an electrochemical split cell technique to evaluate the influence of *Shewanella oneidensis* activities on corrosion of carbon steel. PLoS One 11:e0147899. https://doi.org/10.1371/journal.pone.0147899.
26. Cruz-Garcia C, Murray AE, Klappenbach JA, Stewart V, Tiedje JM. 2007. Respiratory nitrate ammonification by *Shewanella oneidensis* MR-1. J Bacteriol 189:656–662. https://doi.org/10.1128/JB.01194-06.
27. Cheng YF, Niu L. 2007. Mechanisms for hydrogen evolution reaction on pipeline steel in near-neutral pH solution. Electrochem Commun 9:558–562. https://doi.org/10.1016/j.elecom.2006.10.035.
28. Ginner JL, Alvarez PJJ, Smith SL, Scherer MM. 2004. Nitrate and nitrite reduction by Fe^0: influence of mass transport, temperature, and denitrifying microbes. Environ Eng Sci 21:219–229. https://doi.org/10.1089/10928750477308738l.
29. Huang YH, Zhang TC. 2006. Nitrite reduction and formation of corrosion coatings in zerovalent iron systems. Chemosphere 64:937–943. https://doi.org/10.1016/j.chemosphere.2006.01.025.
30. Huang YH, Zhang TC. 2014. Competitive reduction of nitrate, nitrite, and nitrobenzene in Fe^0-water systems. J Environ Eng 140:1306–1315. https://doi.org/10.1061/(ASCE)EE.1943-7870.0000849.
31. Weber KA, Picardal FW, Roden EE. 2001. Microbially catalyzed nitrate-dependent oxidation of biogenic solid-phase Fe(II) compounds. Environ Sci Technol 35:1644–1650. https://doi.org/10.1021/es0016598.
32. Senko JM, Mohamed Y, Dewers TA, Krumholz LR. 2005. Role for Fe(III) minerals in nitrate-dependent microbial U(IV) oxidation. Environ Sci Technol 39:2529–2536. https://doi.org/10.1021/es048906i.
33. Weber KA, Achenbach LA, Coates JD. 2006. Microorganisms pumping iron: anaerobic microbial iron oxidation and reduction. Nat Rev Microbiol 4:752–764. https://doi.org/10.1038/nrmicro1490.
34. Picardal F. 2012. Abiotic and microbial interactions during anaerobic transformations of Fe(II) and NO_x^-. Front Microbiol 3:112. https://doi.org/10.3389/fmicb.2012.00112.
35. Grabb KC, Buchwald C, Hansel CM, Wankel SD. 2017. A dual nitrite isotopic investigation of chemodenitrification by mineral-associated Fe(II) and its production of nitrous oxide. Geochim Cosmochim Acta 196:388–402. https://doi.org/10.1016/j.gca.2016.10.026.
36. Ngala VT, Page CL, Page MM. 2002. Corrosion inhibitor system for remedial treatment of reinforced concrete. Part 1: calcium nitrite. Corros Sci 44:2073–2087. https://doi.org/10.1016/S0010-938X(02)00012-4.
37. Valcarce MB, Vázquez M. 2008. Carbon steel passivity in alkaline solutions: the effect of chloride and nitrite ions. Electrochim Acta 53:5007–5015. https://doi.org/10.1016/j.electacta.2008.01.091.
38. Kim KT, Kim HW, Chang HY, Lim BT, Park HB, Kim YS. 2015. Corrosion inhibiting mechanism of nitrite ion on the passivation of carbon steel and ductile cast iron for nuclear power plants. Adv Mater Sci Eng 2015:408138. https://doi.org/10.1155/2015/408138.
39. Pastore T, Cabrini M, Coppola L, Lorenzi S, Marcassoli P, Buoso A. 2011. Evaluation of the corrosion inhibition of salts of organic acids in alkaline solutions and chloride contaminated concrete. Mater Corros 62:187–195. https://doi.org/10.1002/maco.201005789.
40. Trif L, Shaban A, Telegdi J. 21 February 2018. Electrochemical and surface analytical techniques applied to microbiologically influenced corrosion investigation. Corros Rev https://doi.org/10.1515/corrrev-2017-0032.
41. Rajagopal BS, LeGall J. 1989. Utilization of cathodic hydrogen by hydrogen-oxidizing bacteria. Appl Microbiol Biotechnol 31:406–412. https://doi.org/10.1007/BF00257613.
42. Till BA, Weathers LJ, Alvarez PJJ. 1998. Fe(0)-supported autotrophic chemodenitrification. Environ Sci Technol 32:634–639. https://doi.org/10.1021/es9707769.
43. Iino T, Sakamoto M, Ohkuma M. 2015. *Prolixibacter denitrificans* sp. nov., an iron-corroding, facultatively aerobic, nitrate-reducing bacterium isolated from crude oil, and emended descriptions of the genus *Prolixibacter* and *Prolixibacter bellariivorans*. Int J Syst Evol Microbiol 65:2865–2869. https://doi.org/10.1099/ijs.0.000343.
44. Enning D, Venzlaff H, Garrelfs J, Dinh HT, Meyer V, Mayrhofer K, Hassel AW, Stratmann M, Widdel F. 2012. Marine sulfate-reducing bacteria cause serious corrosion of iron under electroconductive biogenic mineral crust. Environ Microbiol 14:1772–1787. https://doi.org/10.1111/j.1462-2920.2012.02778.x.
45. Chen Y, Tang Q, Senko JM, Cheng G, Zhang Newby B, Castaneda H, Ju L-K. 2015. Long-term survival of *Desulfovibrio vulgaris* on carbon steel and associated pitting corrosion. Corros Sci 90:89–100. https://doi.org/10.1016/j.corsci.2014.09.016.
46. Ross DE, Flynn JM, Baron DB, Gralnick JA, Bond DR. 2011. Towards

electrosynthesis in *Shewanella*: energetics of reversing the Mtr pathway for reductive metabolism. PLoS One 6:e16649. https://doi.org/10.1371/journal.pone.0016649.
47. Choi O, Sang B-I. 2016. Extracellular electron transfer from cathode to microbes: application for biofuel production. Biotechnol Biofuels 9:11. https://doi.org/10.1186/s13068-016-0426-0.
48. Rowe A, Rajeev P, Jain A, Pirbadian A, Okamoto A, Gralnick JA, El-Naggar MY, Nealson KH. 2018. Tracking electron uptake from a cathode into Shewanella cells: implications for energy acquisition from solid-substrate electron donors. mBio 9:e02203-17. https://doi.org/10.1128/mBio.02203-17.
49. Wright MH, Farooqui SM, White AR, Greene AC. 2016. Production of manganese oxide nanoparticles by *Shewanella* species. Appl Environ Microbiol 82:5402–5409. https://doi.org/10.1128/AEM.00663-16.
50. Youssef N, Elshahed MS, McInerney MJ. 2009. Microbial processes in oil fields: culprits, problems, and opportunities. Adv Appl Microbiol 66:141–251. https://doi.org/10.1016/S0065-2164(08)00806-X.
51. Li X, Wang H, Hu C, Yang M, Hu H, Niu J. 2015. Characteristics of biofilms and iron corrosion scales with ground and surface waters in drinking water distribution systems. Corros Sci 90:331–339. https://doi.org/10.1016/j.corsci.2014.10.028.
52. Wang H, Hu C, Han L, Yang M. 2015. Effects of microbial cycling of Fe(II)/Fe(III) and Fe/N on cast iron corrosion in simulated drinking water distribution systems. Corros Sci 100:599–606. https://doi.org/10.1016/j.corsci.2015.08.037.
53. Chen Y, Wang F. 2015. Insights on nitrate respiration by *Shewanella*. Front Mar Sci 1:80. https://doi.org/10.3389/fmars.2014.00080.
54. Usher KM, Kaksonen AH, Cole I, Marney D. 2014. Critical review: microbially influenced corrosion of buried carbon steel pipes. Int Biodeterior Biodegradation 93:84–106. https://doi.org/10.1016/j.ibiod.2014.05.007.
55. Lloyd D. 1993. Aerobic denitrification in soils and sediments: from fallacies to facts. Tree 8:352–356.
56. Burgin AJ, Hamilton SK. 2007. Have we overemphasized the role of denitrification in aquatic ecosystems? A review of nitrate removal pathways. Front Ecol Environ 5:89–96. https://doi.org/10.1890/1540-9295(2007)5[89:HWOTRO]2.0.CO;2.
57. Granger J, Wankel SD. 2016. Isotopic overprinting of nitrification on denitrification as a ubiquitous and unifying feature of environmental nitrogen cycling. Proc Natl Acad Sci U S A 113:E6391–E6400. https://doi.org/10.1073/pnas.1601383113.
58. Ann KY, Jung HS, Kim HS, Moon HY. 2006. Effect of calcium-based corrosion inhibitor in preventing corrosion of embedded steel in concrete. Cem Concr Res 36:530–535. https://doi.org/10.1016/j.cemconres.2005.09.003.
59. Myers CR, Nealson KH. 1990. Respiration-linked proton translocation coupled to anaerobic reduction of manganese(IV) and iron(III) in *Shewanella putrefaciens* MR-1. J Bacteriol 172:6232–62388. https://doi.org/10.1128/jb.172.11.6232-6238.1990.
60. Tanner RS. 2007. Cultivation of bacteria and fungi, p 69–76. *In* Hurst CJ, Crawford RJ, Garland JL, Lipson DA, Mills AL, Stetzenbach LD (ed), Manual of environmental microbiology, 3rd ed. ASM Press, Washington, DC.
61. ASTM International. 2014. Standard guide for electrolytic polishing of metallographic specimens. ASTM E1558-09. ASTM International, West Conshohocken, PA.
62. Giai C, Rincón-Ortiz M, Kappes MA, Senko J, Iannuzzi M. 2016. Efficacy of sterilization methods and their influence on the electrochemical behavior of plain carbon steel. J Electrochem Soc 163:C633–C642. https://doi.org/10.1149/2.0271610jes.
63. ASTM International. 2011. Standard practice for preparing, cleaning, and evaluating corrosion test specimens. ASTM G1-03. ASTM International, West Conshohocken, PA.